analytical chemistry

pubs.acs.org/ac Article

Functionalization of Covalent Organic Frameworks with DNA via Covalent Modification and the Application to Exosomes Detection

Jianyang Lu, Minghui Wang, Yiwei Han, Ying Deng, Yujing Zeng, Chao Li,* Jie Yang,* and Genxi Li*

Cite This: *Anal. Chem.* 2022, 94, 5055−5061 Read Online

ACCESS | Metrics & More | Article Recommendations | Supporting Information

ABSTRACT: The functionalization of covalent organic frameworks (COFs) with biomacromolecules can extend their functions, which is the premise of their application in biomedical research. However, strategies to functionalize COFs with biomacromolecules, which can ensure the stability in complex medium and minimize the undesired effects, are still lacking. In this work, we have proposed a strategy to functionalize COFs with DNA by covalently linking DNA to the functional group on the COF surface through Cu(I)-catalyzed azide/alkyne cycloaddition (CuAAC) reaction. The as-prepared DNA-functionalized COFs (DNA-COFs) can exhibit good hybridization ability and cargo loading ability; thus, we have designed a DNA-COF-based nanoprobe and then fabricated an electrochemical biosensor for the detection of exosomes. In this design, the functionalization with DNA enables COFs to recognize and capture exosomes, and the encapsulation of a large number of methylene blue (MB) in COFs facilitates signal amplification, which can enhance the sensitivity of the biosensor. Moreover, by simply replacing the oligonucleotide sequences, the strategy proposed here can generally be used to build different DNA-COFs with diverse functions for broader biomedical applications.

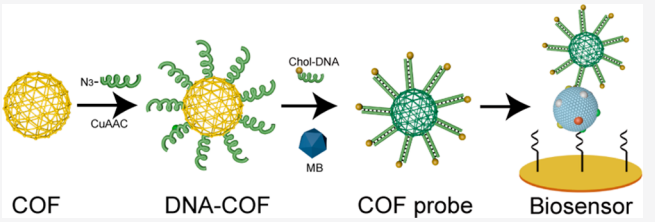

INTRODUCTION

Covalent organic frameworks (COFs), as an emerging kind of porous material built from organic linkers via reversible covalent bond formation, have received extensive attention due to their distinguished properties.[1−4] First, the high specific surface area and tunable nanoscale channels make COFs ideal carriers for cargo loading.[1,2,5,6] Second, a great number of available ligands allow COFs to achieve diverse structures and functions.[3,4] Third, the unsaturated sites of COFs enable them to be postmodified, which can adjust or extend the properties of COFs.[7−9] Furthermore, compared with most nanoparticles, COFs are more biocompatible and less toxic because they are composed of solely light-organic elements.[5,6] The above properties may indicate the great potential of COFs in biomedical applications. However, their biomedical applications are still very limited due to some reasons; for instance, they lack recognition ability for specific biological entities.

To endow nanomaterials with biorecognition ability, biomacromolecules are usually used to functionalize the surface of nanomaterials.[10−12] There are usually three strategies to functionalize nanomaterials with biomacromolecules. The first strategy is the physical adsorption of biomolecules on nanomaterials.[12−14] Due to the weak interaction between nanomaterials and biomacromolecules, the as-prepared nanomaterials usually have poor stability in complex environments. The second strategy is the post-synthetic functionalization of nanomaterials with entities that are amenable to modification of biomacromolecules.[15,16] The introduction of additional units often impacts the intrinsic properties of nanomaterials. So, the third strategy, i.e., covalent modification of the nanomaterials with biomacromolecules will be ideal, which can ensure the stability in complex medium and minimize the undesired effects.[10,11,17] At present, the first two strategies have been used to functionalize COFs,[16,18−22] and thus those functionalized COFs exhibit limited stability or poor homogeneity as well as reduced porosity. To the best of our knowledge, there is still no report to covalently functionalize COFs with biomacromolecules.

Herein, we have first proposed a strategy for covalent modification of COFs with DNA, and then developed an electrochemical biosensor for the detection of exosomes based on the DNA-functionalized COFs (DNA-COFs). Exosomes are an emerging type of biomarkers, which carry more disease information than traditional biomarkers.[23−25] Therefore, exosomes possess a significant detection value, which may help to achieve more accurate and convenient early diagnosis. However, the abundance of exosomes in biofluids is relatively low, which hinders its clinical application. Presently, many methods have been developed for the detection of exosomes, such as enzyme-linked immunosorbent assays (ELISA),

Received: December 2, 2021
Accepted: March 4, 2022
Published: March 15, 2022

https://doi.org/10.1021/acs.analchem.1c05222
Anal. Chem. 2022, 94, 5055−5061

Scheme 1. Schematic Illustration for the Construction of DNA-COFs and Its Application on the Development of Electrochemical Biosensor for the Detection of Exosomes

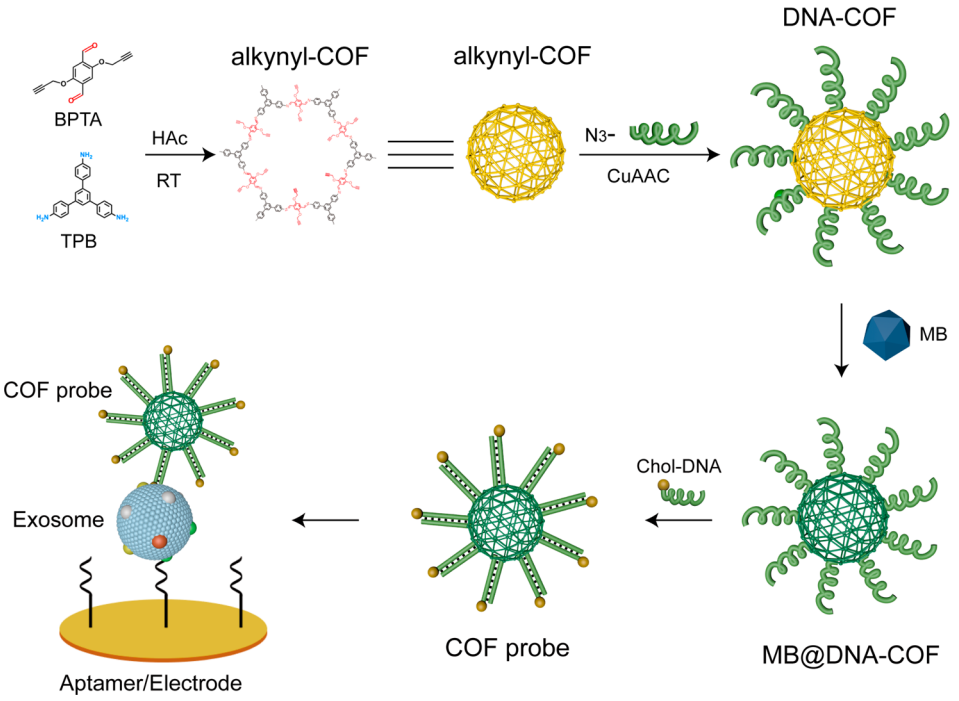

fluorescent assays, colorimetric assays, electrochemical biosensors, and etc.[26−30] Currently, there is an urgent need to develop exosomes detection methods with high sensitivity, high specificity, short detection time, easy operation, and low cost. So, we have also fabricated an electrochemical biosensor for the assay of exosomes by using our prepared DNA-COFs.

EXPERIMENTAL SECTION

Reagents and Apparatus. 1,3,5-Tris(4-aminophenyl)-benzene (TPB) and tris[(1-benzyl-1*H*-1,2,3-triazol-4-yl) methyl] amine (TBTA) were ordered from Aladdin Reagents Co., Ltd. 2,5-Bis(2-propynyloxy) terephthalaldehyde (BPTA) and tetrahydrofuran were purchased from Shanghai Macklin Biochemical Co., Ltd. Tris(2-carboxyethyl) phosphine hydrochloride (TCEP) were obtained from Beyotime Biotechnology Co., Ltd. All oligonucleotides were synthesized and HPLC-purified from Sangon Biotech Co., Ltd. The sequences of oligonucleotides were listed in Table S1. All other reagents were of analytical grade and used without further purification. All solutions were prepared by Millipore water obtained from a Millipore water purification system (Milli-Q, 18.2 MΩ).

The transmission electron microscopy (TEM) images were acquired on a Tecnai G2 F20 S-TWIN instrument (FEI, United States). X-ray diffraction (XRD) patterns were recorded by a D8 Advance diffractometer (Bruker, Germany). Fourier transform infrared (FT-IR) spectroscopy was performed on a NEXUS640 infrared spectrometer (Nicolet, United States). Fluorescence intensity was measured with an F-7000 spectrometer (Hitachi, Japan). The electrochemical measurements were conducted on a CHI660D electrochemical workstation (CH Instruments, USA) with a platinum electrode as the counter electrode, an Ag/AgCl electrode as the reference electrode, and a modified gold electrode as the working electrode.

Synthesis of COFs. COFs containing an alkyne group were synthesized at room temperature according to a previous report with a slight adjustment.[31] Briefly, 70.3 mg of TPB and 72.65 mg of BPTA were dissolved in 25 mL of acetonitrile and mixed by ultrasonic oscillation. Then 2 mL of 12 M acetic acid were added into the mixture and swirled immediately for 10 s. After standing for 72 h, the solution was centrifuged at 10 000 rpm for 10 min to obtain COFs precipitation. The obtained COFs were washed three times with tetrahydrofuran and ethanol and vacuum-dried at 60 °C. The collected COF powder was stored at room temperature for further use.

Functionalization of COFs with DNA. COFs were functionalized with DNA by CuAAC reaction between COFs containing alkyne groups and DNA modified with azide groups. Briefly, 1 mg of COFs was dissolved in 2 mL of CuAAC Buffer (0.5 M NaCl, 50 μM $CuCl_2$, 0.5% DMSO, 1 mM ascorbic acid, 200 μM TBTA, and 1 × PBS), and 20 μL of N_3-DNA were added. The solution was shaken at room temperature for 4 h and then centrifuged at 10 000 rpm for 10 min. The collected precipitate was added to 1 mL 1×PBS containing 1% BSA and allowed to shake for 4 h, followed by centrifugation again at 10 000 rpm for 10 min. The precipitates were washed three times and then dispersed in 1×PBS, and the obtained DNA-COFs were stored at 4 °C for further use.

Hybridization Experiments of DNA-COFs. FAM-labeled DNA (FAM-DNA) was used to verify the successful functionalization of COFs with DNA and its complementary pairing ability. Briefly, 1 μL of 100 μM FAM-DNA was added into 200 μL of DNA-COFs solution (containing 1×PBS, 0.5 M NaCl), and the solution was incubated at room temperature for 1 h. The reaction solution was washed three times with 1×PBS and then suspended in 200 μL of 1×PBS for fluorescence measurement.

Strand displacement assay was then performed. Briefly, 1 μL of 100 μM Competitor DNA was added in 200 μL of DNA-

https://doi.org/10.1021/acs.analchem.1c05222
Anal. Chem. 2022, 94, 5055−5061

COF solution hybridized with FAM-DNA, and the reaction was performed at room temperature for 1 h. Then the reaction solution was washed and dispersed with 1×PBS for fluorescence measurement.

Preparation of COF Probe. To prepare the COF probe, 25 μL of 1 mg/mL MB solution was added in 1 mL of DNA-COFs dissolved in 1×PBS (containing 0.5 M NaCl). The solution was incubated for 24 h before the centrifugation to remove the unloaded MB. Chol-DNA in 1×PBS (containing 0.5 M NaCl) was then added into the precipitate and reacted at room temperature for 1 h. Finally, the mixture was washed three times and then dispersed in 1×PBS to obtain COF probe for further use.

Cell Culture and Exosome Isolation. The medium supernatant of Hela cells was collected and centrifuged at 2000*g* for 20 min to remove large particles such as cell debris. Then the larger vesicles were removed by centrifugation at 10 000*g* for 30 min and ultrafiltration with a pore size of 220 nm. The resulting solution was then centrifuged (120 000*g*, 2 h) to obtain the exosome precipitation. After being suspended with 1×PBS, the obtained exosomes were stored at −80 °C for use and the concentration of exosomes was determined by nanoparticle tracking analysis (NTA).

Electrochemical Detection of Exosomes. Before the detection of exosomes was performed, the gold electrode was treated and modified according to our previous report.[32] The electrode was first soaked in piranha solution for 5 min and polished in turn with 1.0 and 0.3 μm aluminum powders. Then, the electrode was sonicated in ethanol and double-distilled water for 5 min to remove the aluminum powder. Finally, the electrode was scanned by cyclic voltammetry in 0.5 M H_2SO_4 and prepared for use. After being treated with TCEP to reduce disulfide bonds, 10 μL of 1 μM CD63 aptamer were added to the electrode surface and incubated for 1 h. Then the electrode was rinsed with double-distilled water and incubated with 10 μL of 2 mM MCH for 15 min to block the electrode.

To detect exosomes, 10 μL of exosomes were dropped on the aptamer-modified electrode and incubated at room temperature for 2 h. After being rinsed, the electrode was incubated with a 100 μL of COF probe for 1 h. Finally, the electrode was rinsed for electrochemical measurements.

Electrochemical impedance spectra (EIS) were performed in 5 mM $[Fe(CN)_6]^{3-/4-}$ electrolyte containing 1 M KCl with the frequency ranging from 0.1 to 10k Hz. Square wave voltammograms (SWV) were recorded from −0.4 to −0.1 V in PBS. The data were obtained by three parallel measurements.

RESULTS AND DISCUSSION

Principle of the Method. The principle of the functionalization of COFs with DNA and its further application in electrochemical biosensing is illustrated in Scheme 1. The alkynyl-COFs are first synthesized by the condensation of TPB and BPTA at room temperature. Then, the DNA-COFs are synthesized by directly functionalizing azide-DNA on alkynyl-COFs. Specifically, using a Cu(I)-catalyzed azide/alkyne cycloaddition (CuAAC) reaction,[33,34] we have efficiently functionalized clickable alkynyl-containing COFs (alkynyl-COFs) with azide-modified DNA (azide-DNA). Significantly, the DNA-COFs exhibit good hybridization ability and cargo loading ability. Cholesterol-modified DNA has the ability to recognize phospholipid bilayers and is widely used in the isolation and detection of exosomes.[35,36] MB is an excellent redox probe and has been widely employed in the construction of electrochemical biosensors.[37,38] Meanwhile, MB can be adsorbed to a variety of nanomaterials for various applications.[39,40] So, the fabricated DNA-COFs can specifically recognize the exosome membrane after hybridizing with cholesterol-tagged DNA, while the encapsulation of a large number of methylene blue (MB) in COFs facilitates signal amplification, which results in enhanced sensitivity.

To utilize the DNA-COFs in the construction of an electrochemical biosensor, MB is first loaded into DNA-COFs, followed by Chol-DNA hybridization. The affinity of cholesterol to the phospholipid bilayer endows COFs with the ability to target membrane vesicles. The rigid structure of double strands causes cholesterol to have better orientation and improved recognition ability. The biosensor can achieve satisfactory detection performance. Moreover, since no enzyme or additional reaction steps are needed, the fabricated biosensor is simple to operate and easy to store, showing excellent practical application potential. By simply replacing the oligonucleotide sequences, the strategy proposed here to construct DNA-functionalized COFs can also be generally applied in other designs.

Therefore, the prepared COFs have redox reporting ability and phospholipid bilayer targeting ability, so they are denoted as a COF probe. For exosome detection, a CD63 aptamer-immobilized electrode is first prepared to specifically recognize and capture the exosomes via CD63 protein expressed on the surface. Then, the COF probes are introduced onto the electrode surface to form a sandwich structure. So, in the presence of exosomes, a large number of MB loaded in the DNA-COFs can be brought to the electrode surface and generate great enhanced electrochemical response. Therefore, exosomes can be detected and quantified with high sensitivity.

Characterization of DNA-COFs. Transmission electron microscopy (TEM) and scanning electron microscopy (SEM) analysis reveal that the obtained COFs are homogeneous spherical particles with a diameter of 500 nm (Figure 1A, 1B). The powder X-ray diffraction (PXRD) pattern of COFs is consistent with previous studies[31] and reveals that COFs have good crystallinity (Figure 1C). Fourier transform infrared spectroscopy (FT-IR) has been used to characterize the functional groups on the fabricated COFs. As shown in Figure 1E, the FT-IR spectrum has obvious absorption peaks at 3300 and 2150 cm^{-1}, corresponding to the C≡C−H bond and C≡C bond in alkynyl group, respectively. These results indicate that COFs do have an alkynyl group, which may be further used for the functionalization of COFs by DNA molecules.

Further studies reveal that the prepared DNA-COFs have better dispersion in aqueous solution, which can be stable in solution without precipitation (Figures S1 and S2). The reason is that the DNA functionalized on COFs increases the negative charge of COFs, so the solubility of COFs is improved. To prove that, we have measured the zeta potentials of COFs and DNA-COFs. As shown in Figure 1E and Figure S3, the zeta potential of COFs is about −26.5 mV. After functionalization with DNA, the zeta potential of COFs decreases to about −46.5 mV. The nitrogen adsorption−desorption isotherm of the COFs at 77 K has also been performed (Figure 1F). After DNA functionalization, the specific surface area of DNA-COFs decreases from 496 m^2/g to 130 m^2/g and the pore volume decreases from 0.41 cm^3/g to 0.14 cm^3/g. These results indicate the presence of DNA on the COF surface. TEM and SEM images show that the functionalization reaction has negligible damage to the COF particles (Figures S4, S5). The

https://doi.org/10.1021/acs.analchem.1c05222
Anal. Chem. 2022, 94, 5055−5061

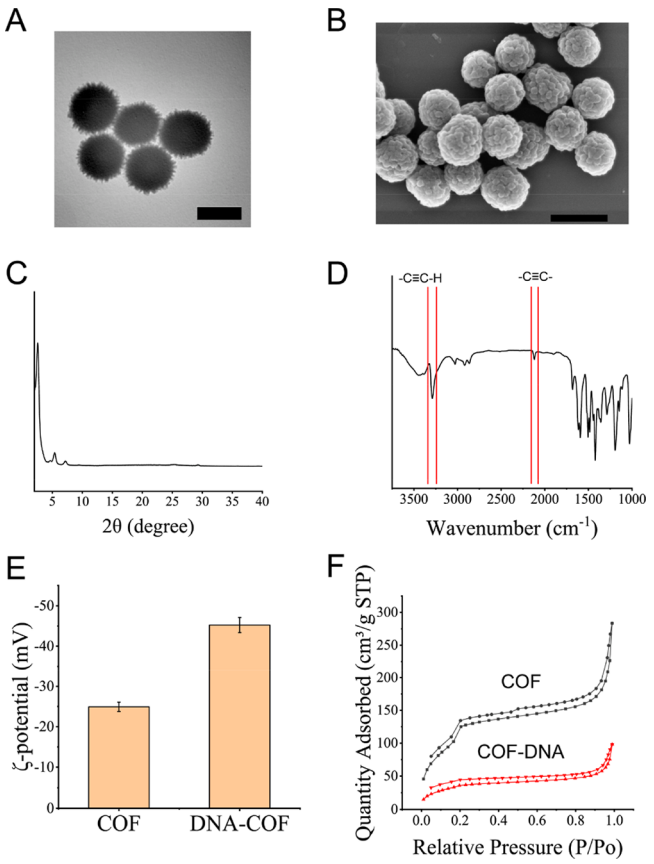

Figure 1. (A) TEM images, (B) SEM images, (C) PXRD pattern, and (D) FT-IR spectra of alkynyl-COFs. Scale bar is 500 nm. (E) ζ-Potential of COFs and DNA-COFs. Error bars represent the standard derivation of three independent experiments. (F) Nitrogen adsorption−desorption isotherm of COFs and DNA-COFs.

DNA-COFs exhibit similar diffraction peaks with COFs in PXRD patterns (Figure S6). All these results indicate the successful functionalization of DNA on the COF surface.

The Hybridization Ability and Cargo Loading Ability of DNA-COFs. Hybridization ability is one of the most appealing characteristics when DNA is used for the functionalization of nanomaterials. Therefore, we have carried out a hybridization experiment to verify the hybridization ability of DNA-COFs. Specifically, we have used a complementary FAM-labeled DNA (FAM-DNA) strand to hybridize with the DNA molecules on COFs surface. We first measured the emission spectrum of DNA-COFs, which shows fluorescence emission in the wavelength range 500−650 nm, while no obvious emission peak at 520 nm can be observed (Figure 2A). However, after hybridization with FAM-DNA, a new fluorescence peak arises at 520 nm, which is attributed to the presence of FAM on the COF surface. In contrast, the emission peak cannot be induced by a noncomplementary FAM-labeled DNA, suggesting the FAM-DNA is sequence-dependent hybridized to the DNA-COF surface. It is worth noting that the DNA-COFs used here and later experiments are passivated by BSA, which can reduce nonspecific adsorption. In fact, the passivation can improve the hybridization ability of DNA (Figure S7). In addition, the fluorescence intensity of DNA-COFs can be modulated by adjusting the functionalization concentration of azide-DNA (Figure 2C) and the hybridization concentration of FAM-DNA (Figure S8). These results imply that our strategy can accurately regulate the number of functional molecules on the surface of COFs.

To further investigate the hybridization ability of DNA-COFs, a DNA strand displacement assay has been carried out. Specifically, a competitor DNA is used to displace the FAM-DNA away from the surface of DNA-COFs, which has a longer complementary sequence to FAM-DNA compared to azide-DNA. As shown in Figure 2C, compared with the FAM-DNA-

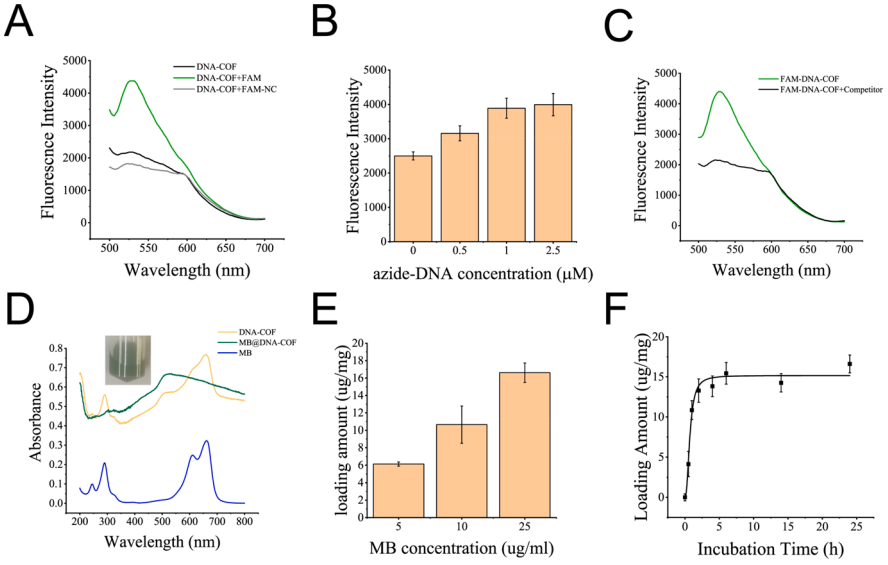

Figure 2. (A) Fluorescence spectroscopy of DNA-COFs, DNA-COF hybridized with FAM-DNA, and DNA-COFs hybridized with noncomplementary FAM-DNA. (B) Relationship between the fluorescence intensity of DNA-COFs hybridized with FAM-DNA and the functionalization concentration of azide-DNA. (C) Fluorescence spectroscopy of FAM-DNA-COFs and FAM-DNA-COFs hybridized with competitor. (D) UV−vis spectroscopy of DNA-COFs, MB, and MB@DNA-COFs. Inset is the photograph of MB@DNA-COFs. (E) The loading amount and the loading ration at different MB concentrations. (F) Relationship between the loading amount and the incubation time. Error bars represent the standard derivation of three independent experiments.

https://doi.org/10.1021/acs.analchem.1c05222
Anal. Chem. 2022, 94, 5055−5061

COFs alone, the fluorescence intensity of FAM-DNA-COFs is significantly decreased by the addition of competitor chains, indicating the DNA-COFs can participate in strand replacement reactions. Indeed, the decrease of fluorescence intensity is concentration-dependent (Figure S9). All the results above indicate that the obtained DNA-COFs possess satisfactory DNA hybridization ability and wide application prospects.

High cargo loading capacity is one of the most important characteristics of COFs in biomedical applications. Therefore, we have explored the cargo-loading capacity of DNA-COFs. In the strategy proposed in this work, additional post-translational modification steps can be avoided, which can maximize the cargo loading capacity of COFs. Methylene blue (MB) is selected as a model cargo molecule because of its wide application in electrochemistry. MB is encapsulated into DNA-COFs by simple incubation, and the unabsorbed MB is removed by centrifugation. The MB-adsorbed DNA-COFs (MB@DNA-COFs) exhibit similar diffraction peaks with COFs in PXRD patterns (Figure S10). An SEM image shows that the functionalization reaction has negligible damage to the COF particles (Figure S11). The specific surface area of MB@DNA-COFs further decreases to 24 m^2/g, and the pore volume decreases to 0.09 cm^3/g (Figure S12). The color of DNA-COFs is changed from yellow to green after the introduction of MB molecules, indicating the successful loading of MB (Figure 2D inset). Meanwhile, DNA-COFs show obvious absorption peaks at 300 and 650 nm after incubation with MB (Figure 2D), which is ascribed to the MB molecules. By measuring the amount of MB in the supernatant after centrifugation, the loading amount of MB within DNA-COFs and the optimal incubation conditions have been evaluated. With the increasing MB concentration, the loading amount of MB increases (Figure 2E). We have also explored the effect of incubation time on MB loading. As is displayed in Figure 2F, the loading amount of MB increases with time in the first few hours and reached a plateau at 5 h. The maximum loading amount is about 16 μg/mg. All the results above indicate that the obtained DNA-COFs possess satisfactory cargo loading capacity.

Feasibility of the Biosensor. Electrochemical impedance spectroscopy (EIS) has been first performed to investigate the stepwise modification of the electrode. As illustrated in Figure 3A, the aptamer-modified Au electrode shows a low electron transfer resistance. After stepwise incubation with exosomes and MB@DNA-COFs, the electrode exhibits gradually increasing diameters of semicircles. It is attributed to the steric hindrance of exosomes and the COF probe, as well as the negative charge of exosomes and the phosphate group of DNAs, proving the successful formation of the sandwich structure on the electrode surface. To verify the feasibility of the fabricated biosensor, the square wave voltammograms (SWV) have been measured. As shown in Figure 3B, the bare electrode and the exosome-free electrode exhibit weak signals.

By contrast, a significant peak is shown in the presence of exosomes. It is because the exosome-mediated proximity of the COF probe to the electrode surface enables MB to generate currents, which confirms the feasibility of this biosensor.

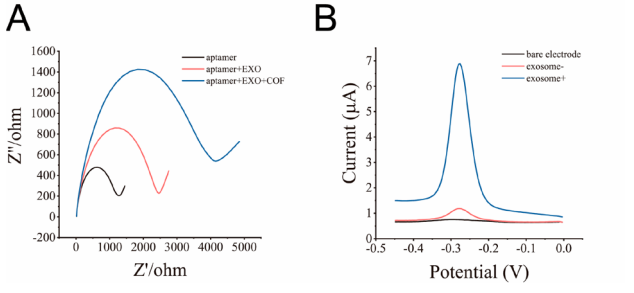

Figure 3. (A) EIS corresponding to the stepwise treatment of the electrode. Electrode modified with aptamer (black curve), after incubation with exosomes (red curve), and further incubation with COF-probe (blue curve). (B) SWV responses obtained on the cases with bare electrode (black curve), exosomes-free (red curve), and 1.0 × 10^7 particles/μL exosomes (blue curve).

Detection Performance. To improve the performance of the biosensor, the concentration of the COF probe has been optimized. As displayed in Figure S13, enhanced electrochemical signal can be observed with the increase of the concentration of COF probe, and 0.5 mg/mL is chosen as the optimal concentration.

We have employed the DNA-COF-based biosensor to quantitatively analyze different concentrations of target exosomes. As illustrated in Figure 4A, the current response

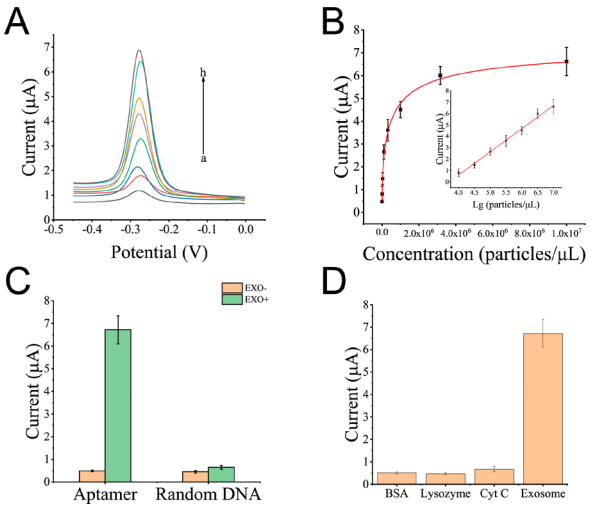

Figure 4. (A) SWV responses of electrochemical biosensor at different concentrations of exosomes. a–h: 0, 10^4, 3.16 × 10^4, 10^5, 3.16 × 10^5, 10^6, 3.16 × 10^6, 10^7 particles/μL. (B) Relationship between the values of peak current and the exosome concentrations. Inset is the linear range. (C) Peak current corresponding to the biosensor modified with exosome aptamer or random single strand DNA. (D) Peak current corresponding to the biosensor treated with BSA, lysozyme, Cyt C, and exosome. Error bars represent the standard derivation of three independent experiments.

increases correspondingly with the concentration of exosomes. A linear relationship between the current response and the logarithmic value of exosomes concentrations ranging from 10^4 to 10^7 particles/μL can be established (Figure 4B). The linear equation is I = 2.04 lgc − 7.56 with a correlation coefficient of 0.9919. The limit of detection is calculated as 9661 particles/μL based on the average of the background signal plus 3 times the standard deviation, indicating the satisfactory sensitivity of the fabricated biosensor.

The specificity of this biosensor for exosomes detection has been also evaluated. The specificity of the biosensor is mainly achieved by the specific binding of CD63 aptamer to CD63 protein on the surface of exosomes. Therefore, we have employed a random single-strand DNA to replace the CD63

https://doi.org/10.1021/acs.analchem.1c05222
Anal. Chem. 2022, 94, 5055−5061

aptamer on the electrode and observed the signal response. As shown in Figure 4C, no significant signal is observed in the presence of exosomes when a random single-strand DNA is modified on the electrode surface, suggesting that this biosensor has good selectivity toward exosomes with high expression of CD63. We have also tested the specificity of the biosensor by several proteins, such as BSA, lysozyme, and Cyt C, and the biosensor also exhibits good selectivity (Figure 4D).

The reproducibility of the biosensor has been tested by deploying six independent biosensors for exosomes quantification. The relative standard deviation (RSD) value for the six biosensors is 2.0%, indicating the good reproducibility of the biosensor (Figure S14). The electrochemical biosensor can be reused by washing the electrode at 95 °C with minor signal loss (Figure S15). We have also tested the durability of COF probes. After 2 weeks of storage, the PXRD patterns, SEM image, and nitrogen adsorption−desorption isotherm of COF probes shows no significant change (Figures S16, S17, S18). And the COF probe shows only slight signal loss after 2 weeks of storage at 4 °C (Figure S19), indicating the good durability of COF probes.

Determination of Exosomes in Complex Environments. To deploy in practical applications, electrochemical biosensors must be able to withstand the challenge of complex medium. To validate the application potential of the proposed biosensor, the anti-interference ability of the biosensor in complex environments has been tested. Figure 5 shows the

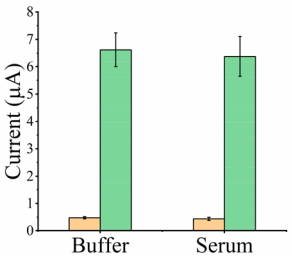

Figure 5. Values of peak current at buffer and serum without and with exosomes. The serum used here was 10% ultracentrifuged fetal bovine serum. Error bars represent the standard derivation of three independent experiments.

detection performance of the sensor in 10% human serum and buffer. No significant difference is observed, whether the target exosomes are presented. The above results demonstrate that our biosensor works well in complex biological samples and has the potential for clinical diagnosis.

CONCLUSIONS

In this work, we have realized the nucleic acid functionalization of COFs for the first time by modifying the azide-tagged DNA onto alkynyl-containing COFs through the CuAAC reaction. Our strategy to functionalize COFs possesses several advantages. First, the CuAAC reaction is robust and highly efficient under ambient conditions, which causes little damage to functional biomolecules. Second, the reaction between an alkyne- and azide-terminated molecule is orthogonal, which can achieve site-specific immobilization of biomacromolecules on the surface of COFs. Third, directly functionalizing DNA on COF ligands can minimize the impact on the characteristics of COFs. Fourth, the strategy can maintain the uniform distribution of DNA on the surface of COFs. So, the obtained DNA-COFs possess satisfactory DNA hybridizing ability and cargo loading ability, which can be used to design COF probes. The COF probes have further been used to construct an effective electrochemical biosensor for the detection of exosomes by forming a sandwich structure. Therefore, the nucleic acid functionalized COFs have been proven to possess great potential for biomedical applications. We believe that more properties of DNA-COFs will be explored, as well as its applications. Additionally, more types of functionalized COFs can be developed by changing the sequence of modifying DNA to extend their functions and applications.

ASSOCIATED CONTENT

Supporting Information

The Supporting Information is available free of charge at https://pubs.acs.org/doi/10.1021/acs.analchem.1c05222.

Oligonucleotides used in this work; characterization of COFs, DNA-COFs, MB@DNA-COFs; DNA hybridization experiments of DNA-COFs; optimization of the biosensor; the repeatability, reusability, and durability of the biosensor. (PDF)

AUTHOR INFORMATION

Corresponding Authors

Chao Li − *School of Food and Biological Engineering, Hefei University of Technology, Hefei, Anhui 230009, P. R. China;* orcid.org/0000-0002-2552-413X; Email: lchao@hfut.edu.cn

Jie Yang − *State Key Laboratory of Pharmaceutical Biotechnology, School of Life Sciences, Nanjing University, Nanjing 210023, P. R. China*; Email: yangjie@nju.edu.cn

Genxi Li − *State Key Laboratory of Pharmaceutical Biotechnology, School of Life Sciences, Nanjing University, Nanjing 210023, P. R. China; Center for Molecular Recognition and Biosensing, School of Life Sciences, Shanghai University, Shanghai 200444, P. R. China;* orcid.org/0000-0001-9663-9914; Email: genxili@nju.edu.cn

Authors

Jianyang Lu − *State Key Laboratory of Pharmaceutical Biotechnology, School of Life Sciences, Nanjing University, Nanjing 210023, P. R. China*

Minghui Wang − *State Key Laboratory of Pharmaceutical Biotechnology, School of Life Sciences, Nanjing University, Nanjing 210023, P. R. China*

Yiwei Han − *State Key Laboratory of Pharmaceutical Biotechnology, School of Life Sciences, Nanjing University, Nanjing 210023, P. R. China*

Ying Deng − *State Key Laboratory of Pharmaceutical Biotechnology, School of Life Sciences, Nanjing University, Nanjing 210023, P. R. China*

Yujing Zeng − *State Key Laboratory of Pharmaceutical Biotechnology, School of Life Sciences, Nanjing University, Nanjing 210023, P. R. China*

Complete contact information is available at: https://pubs.acs.org/10.1021/acs.analchem.1c05222

Notes

The authors declare no competing financial interest.

https://doi.org/10.1021/acs.analchem.1c05222
Anal. Chem. 2022, 94, 5055−5061

■ ACKNOWLEDGMENTS

This work is supported by the National Natural Science Foundation of China (Grant No. 81772593) and the Fundamental Research Funds for the Central Universities (Grant No. 14380163).

■ REFERENCES

(1) Côté, A. P.; Benin, A. I.; Ockwig, N. W.; O'Keeffe, M.; Matzger, A. J.; Yaghi, O. M. *Science* **2005**, *310* (5751), 1166−1170.
(2) Xu, H.; Gao, J.; Jiang, D. *Nat. Chem.* **2015**, *7* (11), 905−912.
(3) Lohse, M. S.; Bein, T. *Adv. Funct. Mater.* **2018**, *28* (33), 1705553.
(4) Geng, K.; He, T.; Liu, R.; Dalapati, S.; Tan, K. T.; Li, Z.; Tao, S.; Gong, Y.; Jiang, Q.; Jiang, D. *Chem. Rev.* **2020**, *120* (16), 8814−8933.
(5) Fang, Q.; Wang, J.; Gu, S.; Kaspar, R. B.; Zhuang, Z.; Zheng, J.; Guo, H.; Qiu, S.; Yan, Y. *J. Am. Chem. Soc.* **2015**, *137* (26), 8352−8355.
(6) Ge, L.; Qiao, C.; Tang, Y.; Zhang, X.; Jiang, X. *Nano Lett.* **2021**, *21* (7), 3218−3224.
(7) Sun, Q.; Aguila, B.; Perman, J.; Earl, L. D.; Abney, C. W.; Cheng, Y.; Wei, H.; Nguyen, N.; Wojtas, L.; Ma, S. *J. Am. Chem. Soc.* **2017**, *139* (7), 2786−2793.
(8) Yusran, Y.; Guan, X.; Li, H.; Fang, Q.; Qiu, S. *Natl. Sci. Rev.* **2020**, *7* (1), 170−190.
(9) Fan, H.; Peng, M.; Strauss, I.; Mundstock, A.; Meng, H.; Caro, J. *Nat. Commun.* **2021**, *12* (1), 38.
(10) Liu, J.; Lu, Y. *Nat. Protoc* **2006**, *1* (1), 246−252.
(11) Miller, B. S.; Bezinge, L.; Gliddon, H. D.; Huang, D.; Dold, G.; Gray, E. R.; Heaney, J.; Dobson, P. J.; Nastouli, E.; Morton, J. J. L.; McKendry, R. A. *Nature* **2020**, *587* (7835), 588−593.
(12) Yao, G.; Li, J.; Li, Q.; Chen, X.; Liu, X.; Wang, F.; Qu, Z.; Ge, Z.; Narayanan, R. P.; Williams, D.; Pei, H.; Zuo, X.; Wang, L.; Yan, H.; Feringa, B. L.; Fan, C. *Nat. Mater.* **2020**, *19* (7), 781−788.
(13) Röder, R.; Preiß, T.; Hirschle, P.; Steinborn, B.; Zimpel, A.; Höhn, M.; Rädler, J. O.; Bein, T.; Wagner, E.; Wuttke, S.; Lächelt, U. *J. Am. Chem. Soc.* **2017**, *139* (6), 2359−2368.
(14) Wang, S.; McGuirk, C. M.; Ross, M. B.; Wang, S.; Chen, P.; Xing, H.; Liu, Y.; Mirkin, C. A. *J. Am. Chem. Soc.* **2017**, *139* (29), 9827−9830.
(15) Shao, F.; Zhang, L.; Jiao, L.; Wang, X.; Miao, L.; Li, H.; Zhou, F. *Anal. Chem.* **2018**, *90* (14), 8673−8679.
(16) Shao, K.; Wang, B.; Nie, A.; Ye, S.; Ma, J.; Li, Z.; Lv, Z.; Han, H. *Biosens. Bioelectron* **2018**, *118*, 160−166.
(17) Morris, W.; Briley, W. E.; Auyeung, E.; Cabezas, M. D.; Mirkin, C. A. *J. Am. Chem. Soc.* **2014**, *136* (20), 7261−7264.
(18) Deng, X.; Fang, Y.; Lin, S.; Cheng, Q.; Liu, Q.; Zhang, X. *ACS Appl. Mater. Interfaces* **2017**, *9* (4), 3514−3523.
(19) Zhang, T.; Ma, N.; Ali, A.; Wei, Q.; Wu, D.; Ren, X. *Biosens. Bioelectron* **2018**, *119*, 176−181.
(20) Feng, S.; Yan, M.; Xue, Y.; Huang, J.; Yang, X. *Anal. Chem.* **2021**, *93* (40), 13572−13579.
(21) Gao, P.; Tang, K.; Lou, R.; Liu, X.; Wei, R.; Li, N.; Tang, B. *Anal. Chem.* **2021**, *93* (35), 12096−12102.
(22) Hu, W.-C.; Pang, J.; Biswas, S.; Wang, K.; Wang, C.; Xia, X.-H. *Anal. Chem.* **2021**, *93* (24), 8544−8552.
(23) Salehi, M.; Sharifi, M. *J. Cell. Physiol* **2018**, *233* (9), 6370−6380.
(24) Console, L.; Scalise, M.; Indiveri, C. *Clin. Chim. Acta* **2019**, *488*, 165−171.
(25) Hadavand, M.; Hasni, S. *Oral Dis* **2019**, *25* (1), 10−15.
(26) Liu, C.; Xu, X.; Li, B.; Situ, B.; Pan, W.; Hu, Y.; An, T.; Yao, S.; Zheng, L. *Nano Lett.* **2018**, *18* (7), 4226−4232.
(27) Wang, L.; Pan, Y.; Liu, Y.; Sun, Z.; Huang, Y.; Li, J.; Yang, J.; Xiang, Y.; Li, G. *ACS Appl. Mater. Interfaces* **2020**, *12* (1), 322−329.
(28) Wang, S.; Zhang, L.; Wan, S.; Cansiz, S.; Cui, C.; Liu, Y.; Cai, R.; Hong, C.; Teng, I. T.; Shi, M.; Wu, Y.; Dong, Y.; Tan, W. *ACS Nano* **2017**, *11* (4), 3943−3949.
(29) Sun, Z.; Wang, L.; Wu, S.; Pan, Y.; Dong, Y.; Zhu, S.; Yang, J.; Yin, Y.; Li, G. *Anal. Chem.* **2020**, *92* (5), 3819−3826.
(30) Wang, M.; Pan, Y.; Wu, S.; Sun, Z.; Wang, L.; Yang, J.; Yin, Y.; Li, G. *Biosens. Bioelectron* **2020**, *169*, 112638.
(31) Ma, W.; Zheng, Q.; He, Y.; Li, G.; Guo, W.; Lin, Z.; Zhang, L. *J. Am. Chem. Soc.* **2019**, *141* (45), 18271−18277.
(32) Han, Y.; Zhang, Y.; Wu, S.; Jalalah, M.; Alsareii, S. A.; Yin, Y.; Harraz, F. A.; Li, G. *ACS Appl. Mater. Interfaces* **2021**, *13* (31), 36919−36925.
(33) Wang, P.; Silverman, S. K. *Angew. Chem.-Int. Edit* **2016**, *55* (34), 10052−10056.
(34) Zheng, W.; Li, H.; Chen, W.; Zhang, J.; Wang, N.; Guo, X.; Jiang, X. *Small* **2018**, *14* (14), 1703857.
(35) Yang, Y.; Wu, Z.; Wang, L.; Zhou, K.; Xia, K.; Xiong, Q.; Liu, L.; Zhang, Z.; Chapman, E. R.; Xiong, Y.; Melia, T. J.; Karatekin, E.; Gu, H.; Lin, C. *Nat. Chem.* **2021**, *13*, 335−342.
(36) Jiang, Y.; Shi, M.; Liu, Y.; Wan, S.; Cui, C.; Zhang, L.; Tan, W. *Angew. Chem.-Int. Edit* **2017**, *56*, 11916−11920.
(37) Fan, C. H.; Plaxco, K. W.; Heeger, A. J. *Proc. Natl. Acad. Sci. U. S. A* **2003**, *100*, 9134−9137.
(38) Li, C.; Hu, X. L.; Lu, J. Y.; Mao, X. X.; Xiang, Y.; Shu, Y. Q.; Li, G. X. *Chem. Sci.* **2018**, *9*, 979−984.
(39) Sun, Z. W.; Wang, L.; Wu, S.; Pan, Y. H.; Dong, Y.; Zhu, S.; Yang, J.; Yin, Y. M.; Li, G. X. *Anal. Chem.* **2020**, *92*, 3819−3826.
(40) Jia, X.; Bai, J.; Ma, Z.; Jiang, X. *J. Mater. Chem. B* **2017**, *5*, 269−278.

https://doi.org/10.1021/acs.analchem.1c05222
Anal. Chem. 2022, 94, 5055−5061